SSC24-WIV-09

Design and development of 2U SPIRONE CubeSat for verification of navigation signal generator in LEO environment and marine plastic observation

Sunhwan Gwon, Pilkyo Jeong, Hyewon Park, Ah-yeon Park, Minji kim, Kihyun Kim, Hyewon Jo, Hyung-Goo Lim, Ina Jeong, Ahn Doeun, Hyunjung Kim, Lee Hoonseok, O-Jong Kim (ojong@sejong.ac.kr)
Department of Aerospace Systems Engineering, Sejong University
1118, Chungmugwan, 209, Neungdong-ro, Gwangjin-gu, Seoul, Republic of Korea; +821041779244
accman3@sju.ac.kr

ABSTRACT

This study aims to undertake the development of the SPIRONE Cube-satellite. The technical mission involves the development and validation of an S-band navigation signal generator for Low Earth Orbit (LEO), and the scientific mission is to observe marine plastics using Long-Wave Infrared (LWIR) and Short-Wave Infrared (SWIR) cameras. Traditional satellite navigation systems operate at medium Earth orbits around 20,000 km, where signals can weaken and become vulnerable to interference, impacting air navigation, shipping, and autonomous vehicles, potentially causing severe accidents. To address this, the project aims to explore LEO-based navigation by operating CubeSats in LEO to collect experimental data and conduct related research. Additionally, the CubeSat is equipped with LWIR and SWIR cameras to detect and help remove plastics in specific ocean areas. The SPIRONE CubeSat weighs approximately 2.48 kg [TBD] with a one-year mission duration, operating in a sun-synchronous orbit at 600km altitude. The onboard computer (OBC) uses FreeRTOS, and the satellite's hardware and subsystems are integrated for synchronized missions with the ground station. Simulation-based structural analysis, including random vibration and modal analysis, as well as shock tests, were conducted. In addition, simulation-based thermal analysis was conducted to assess the feasibility of mission execution in the target orbit. Power production was estimated considering the Noon-Midnight Orbit, ensuring sufficient margin. The ground station will be developed and utilized in-house, and there is also a plan to utilize the ground station of the Korea Aerospace Research Institute (KARI). Ham Radio Deluxe will be used for satellite control software, and in-house development is underway for satellite communication software. Additionally, through link budget analysis, it has been confirmed that there is sufficient margin. The SPIRONE CubeSat project conducted the Critical Design Review (CDR) in October 2023 and confirmed the design through the delta CDR in March 2024. Ultimately, it will be loaded onto the Nuri Rocket in 2025, and its mission execution and verification will be carried out in the LEO environment.

INTRODUCTION

The SPIRONE CubeSat of Sejong University was selected in the basic satellite category at the 2022 CubeSat Competition hosted by KARI and is currently in the development stage. This CubeSat is a standard 2U CubeSat and is planned to be launched along with the Nuri rocket's 4th launch (scheduled for November 2025) to achieve a sun-synchronous orbit at an altitude of 600 km and an inclination of 97.8 degrees. The SPIRONE CubeSat has two main missions. The first is a technical mission to develop and verify a LEO navigation signal generator onboard. The second is a scientific mission to observe marine plastic waste using a SWIR camera and an LWIR camera. The overall structure of this paper will first introduce the mission operation concept and the general system architecture of the CubeSat. Following this, the current development processes of each subsystem will be briefly discussed, concluding the paper.

MISSION OPERATION CONCEPT

Technical mission

A CubeSat equipped with a satellite navigation signal generator can be utilized for research on LEO satellite navigation systems. Navigation satellites of conventional satellite navigation systems such as GPS, Galileo, GLONASS, and Beidou are operated in medium Earth orbit (MEO) at an altitude of approximately 20,000 km. These existing satellite navigation systems have a limitation of being vulnerable to radio-frequency interference (RFI) such as jamming and spoofing due to the very weak signal strength received on Earth. This issue adversely affects systems relying on satellite navigation, such as aviation, maritime, and autonomous vehicles, and can lead to disaster-level accidents, such as aircraft crashes, in severe cases. In contrast, LEO-based

navigation satellites have the advantage of being closer to Earth, which allows for stronger transmission power of navigation signals and greater resilience to RFI[1]. They can also serve as backup navigation systems in the event of jamming or spoofing incidents.

For these reasons, attempts have been made to calculate positions using satellites operating in LEO. Research has been conducted to perform positioning using Iridium satellites[2] or by measuring the Doppler shift of SpaceX's Starlink signals[3], and OneWeb satellites are also being considered for their functionality as navigation satellites. In addition, NewSpace companies such as Xona Space Systems, Satelles, and Trustpoint are actively participating in the development of their own LEO PNT (Position, Navigation, and Timing) systems[4,5].

The primary technical goal of this CubeSat project is to develop a navigation signal generator payload to provide positioning services in the LEO environment and to verify it in low Earth orbit. This project aims to obtain experimental data related to LEO navigation and conduct relevant research, including analyzing the unique dynamical characteristics of the LEO environment and differences from MEO navigation satellites. For broadcasting navigation signals, the plan is to use the 2.4 GHz S-band amateur radio frequency range, which does not overlap with GNSS (Global Navigation Satellite System) signals. The payload verification will be carried out through a successful GPS time synchronization scenario using a single CubeSat or simultaneous reception with ground broadcasting equipment. This verification is expected to contribute to the establishment of LEO navigation systems.

Scientific mission

As societal interest in environmental issues increases, attention is also growing regarding the pollution of the oceans, which cover 70% of the Earth's surface and contain 97% of its water resources. Notably, as of 2023, the size of the Great Pacific Garbage Patch is estimated to be around 1.4 million km^2, approximately twice the area of the state of Texas, and this marine plastic pollution is having a severe impact on the marine ecosystem[6].

Plastics released into the natural environment, including the oceans, are known to persist for approximately 100 years, posing a significant threat not only to humans but to all life on Earth. Since the severity of marine plastic pollution became apparent, various methods have been attempted to collect plastic, including direct beach cleanups by individuals and the deployment of large-scale V-shaped structures floating on the surface to trap plastic, as utilized by The Ocean Cleanup Initiative. However, to implement these methods effectively, it is necessary to assess the current status of plastic waste in the oceans.

Therefore, the development of marine plastic detection technology is crucial for the removal of marine plastic. The scientific mission of the SPIRONE CubeSat aims to observe and locate marine plastics in the Korean Peninsula and the Pacific/Atlantic oceans using SWIR and LWIR cameras, facilitating their removal. To achieve this objective, the CubeSat will be equipped with an infrared camera array to observe marine plastic waste.

System operation

The SPIRONE satellite system operates in a total of 7 modes, with the roles of each operation mode summarized as shown in Table 1. The satellite's system operation involves transitions between each mode. After completing the initial mode, it enters a standby mode to receive commands from the ground station, continuously monitoring battery levels and ground station commands to transition to each mode or safety mode as necessary. Flight software block diagrams for each mode are summarized as shown in Figure 1.

Table 1: Operational Modes and Role

Operation mode	Operational role
Initial	From Pod separation until satellite stabilization
Standby	Immediately after initial mode, awaiting ground station command or mission completion
Technical mission	During overflights of the Korean peninsula, broadcast LEO navigation signals to technically validate the LEO navigation signal generator
Scientific mission	Observe marine plastic pollution over the Korean peninsula, Atlantic, and Pacific using the IR camera array during orbital passes
Communication	Downlink mission data to ground station via UHF communications
Safe	Perform when battery low, system malfunction, or OBC reboot needed
Hibernation	Perform end of mission operations

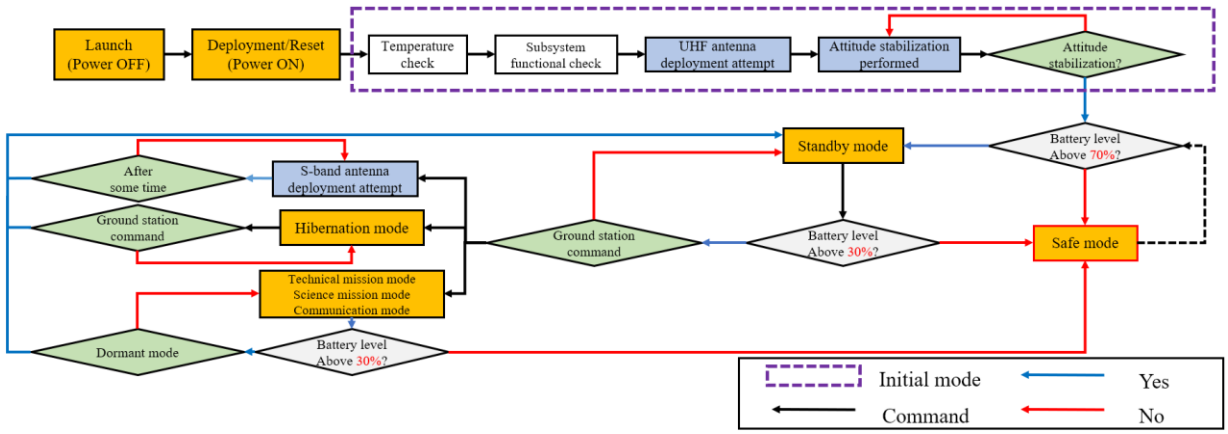

Figure 1: Flight Software Block Diagram

SYSTEM ARCHITECTURE DEFINITION

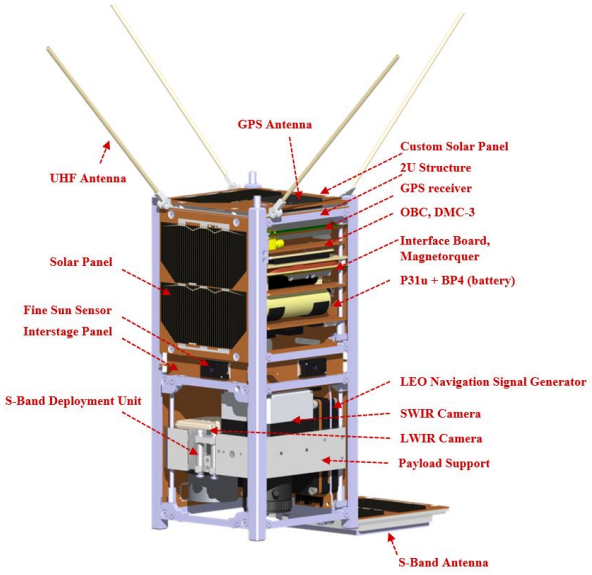

Figure 2: SPIRONE Cubesat System Overview

The overall configuration of the SPIRONE CubeSat is shown in Figure 2. The payload includes a LEO navigation signal generator for generating navigation signals in the LEO environment and an IR camera array in the IR band for detecting marine plastics. Additionally, the GPS antenna will be placed on the top surface along with a custom solar panel. This custom solar panel is also planned to accommodate an additional Fine Sun Sensor (FSS). Furthermore, for attitude determination and control, four additional FSS and a 3-axis Magnetorquer will be deployed. Additionally, a UHF antenna capable of both transmission and reception will be installed to facilitate smooth communication with ground stations.

The structure of the SPIRONE CubeSat will utilize a 2U form factor. The engineering model (EM) was fabricated through hard anodizing by a domestic aluminum processing company. For the flight model (FM), a 2U structure from ISIS, known for its flight heritage, will be used. The power system includes modules related to the battery, comprising the NanoPower P31u Board and NanoPower BP4 from Gomspace. There are a total of four batteries and two battery heaters. Solar panels for power generation will be from the NanoPower P110 Series.

OBC will be the NanoMind A3200, and the UHF transceiver will be the NanoCom AX100 module, both mounted on the NanoDock DMC-3 board. The OBC will manage payloads such as the LEO navigation signal generator, LWIR camera, SWIR camera, GPS receiver, Fine Sun Sensor, magnetometer, communication, and power systems. Attitude control modules include the Z-axis magnetorquer and X, Y-axis magnetorquers from CubeSpace. For sun position sensing, the FSS from Gomspace will be used.

The interstage panel, which connects the satellite's external and internal components and serves as the UHF antenna's mounting point, will use the NanoUtil GSSB module. Communication will be handled by the NanoCom ANT430 UHF antenna for both transmission and reception. For navigation signal broadcasting, a 2.4 GHz S-Band antenna will be used to avoid overlap with existing GNSS signals. The GPS antenna will be integrated with the custom solar panel on the CubeSat's top surface.

The overall system interface of the SPIRONE CubeSat is depicted in Figure 3.

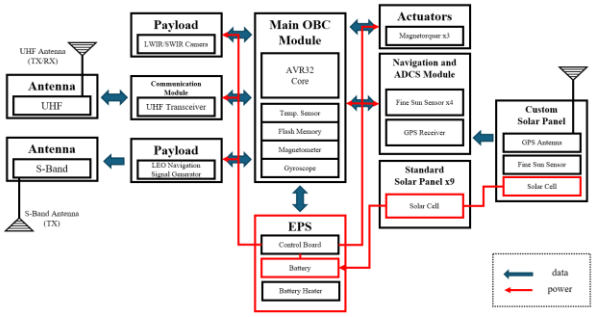

Figure 3: SPRIONE CubeSat System Interface

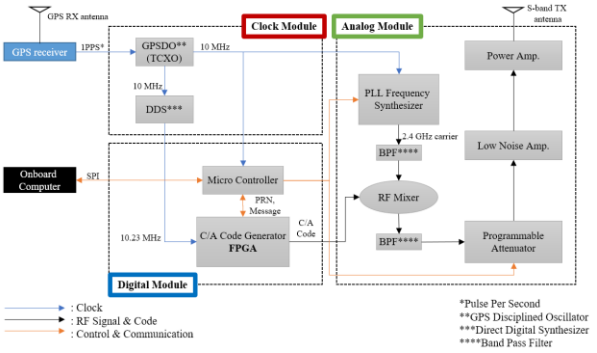

Figure 4: LEO Navigation Generator Hardware Block Diagram

PAYLOAD AND SATELLITE SUBSYSTEMS

LEO Navigation Signal Generator

A notable product generating navigation signals in the 2.4 GHz band is the LocataLite by Locata, Australia[7]. LocataLite is a pseudolite that broadcasts navigation signals at 2.4 GHz from Locata ground stations installed on the ground. It serves as a navigation signal generator installed on multiple ground stations in an area to provide position information similar to satellite navigation systems. In this CubeSat project, the aim is to develop a navigation signal generator that can be installed on CubeSat platforms for operation in the LEO environment, considering the signal specifications of LocataLite broadcasting in the 2.4 GHz band, and verify it in actual orbit. The signal specifications of LocataLite are designed similarly to GPS L1 C/A specifications. It employs CDMA (Code-division-multiple-access) technique using spreading codes, and each satellite applies different PRN (Pseudo Random Noise) to distinguish signal sources. The difference between LocataLite and GPS L1 C/A lies in the chipping rate, which is 10.23 Mcps instead of 1.023 Mcps, and the C/A code cycle is 100us instead of 1ms.

The navigation signal generator being developed is designed to the same specification as the GPS L1 C/A signal. The carrier signal will apply the same BPSK (Bi-Phase Shift Key) modulation as LocataLite and GPS L1 C/A, and plans are to accommodate the C/A code. The navigation message is constructed with a data rate of 50 bps and can be expedited to 250 and 500 bps, taking into consideration constraints on communication time. The navigation signal generator is being considered for development based on FPGA (Field Programmable Gate Array), and the overall block diagram of the designed navigation signal generator is shown in Figure 4.

IR camera array

The scientific mission of this CubeSat project is to utilize CubeSat in low Earth orbit with SWIR and LWIR band cameras, which have flight heritage, for the purpose of detecting macroplastics in the ocean. Remote sensing of marine macroplastic debris has been extensively studied and implemented in the visible (VIS), near-infrared (NIR), and short-wave infrared (SWIR) wavelength bands. Recent research efforts have focused on thermal infrared detection to complement observations in the VIS-SWIR wavelength range[8]. Thermal infrared detection primarily occurs in the mid-wave infrared (MWIR) and long-wave infrared (LWIR) wavelength bands, observing infrared emitted from objects rather than measuring reflected light as in VIS-SWIR wavelength observations[9].

Table 2: Comparative Analysis of Infrared (IR) Camera Array Characteristics

	SWIR Camera	LWIR Camera
Plastic type classification	○	△
Visible-light imagery	Similar	Dissimilar
Elusive plastics	Dark colored	High emissivity, High specific heat
Sensor noise	Relatively low	Relatively high
Nighttime imaging	Difficulty	Possible
Overcast day photography	Difficulty	Possible
Advantage	Accuracy, Reliability	Stability, Sustainability

When using SWIR and LWIR cameras simultaneously, exploiting these contrasting characteristics allows for more detailed plastic detection compared to using a single band alone. By confirming the presence of plastic using LWIR cameras, then capturing the area with SWIR cameras, it's possible to classify the type of plastic in

finer detail or obtain imagery closer to visible light. Additionally, in the absence of light sources over the sea, which makes SWIR camera capture difficult at night, LWIR cameras can be utilized to acquire nighttime data. While observation with LWIR cameras can be challenging when there's not a significant temperature difference between seawater and the atmosphere, SWIR cameras enable plastic detection regardless of temperature. Moreover, while LWIR cameras may struggle to distinguish between plastic and other marine floating debris, comparison with SWIR camera data can aid in identifying plastics specifically.

Figure 5 illustrates the scientific mission scenario process in an easily understandable manner. Due to their large size, RAW images are initially compressed into smaller JPEG files by the OBC. To ensure matching between RAW images and JPEG files, information such as file sizes and lists of captured RAW images and JPEG files are stored in a log file. Subsequently, the compressed JPEG files and log information are downlinked to the ground. Upon receiving the files, a selection is made among the images to be downlinked again in RAW format. Using the information from the log file, a downlink telecommand containing the selected RAW image list is transmitted. Upon receiving the command, the OBC proceeds to transmit the RAW images to the ground.

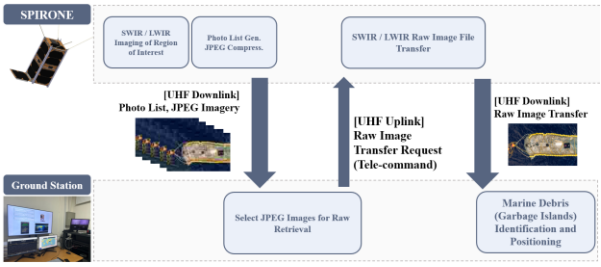

Figure 5: Scientific Mission Scenario

GPS receiver

In this CubeSat, the role of the GPS receiver extends beyond calculating and providing satellite position and timing information; it also ensures that the LEO navigation signal generator payload can generate signals synchronized with GPS system Time. To achieve this, a GPS receiver with successful space operation and Flight Heritage must be installed. The GPS receiver to be installed on the SPIRONE CubeSat has been previously flown and verified on the SNUGLITE-I. The SNUGLITE-I had successfully verified the L1/L2C dual-frequency GPS receiver in orbit for more than a year[10]. The characteristics of the developed receiver are depicted in Figure 6, and its specifications are detailed in Table 3.

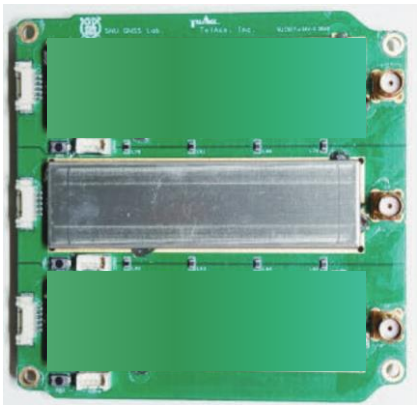

Figure 6: GPS Receiver

Table 3: GPS Receiver Specifications

Specifications	
Operating Voltage	3.3V
Power Consumption (per receiver)	L1: 340mW L1/L2C: 450mW
Operating Temperature	-40 ~ +85℃
Mass	165.5 g (3 receivers)
Size	PC/104 Form Factor (2 Receivers)
Interface	UART (3.3v-level)
Tracking Channels	Maximum 24 Channels

The key component, the GPS L1/L2 Baseband chip, is a chip developed in-house by a domestic company, with all components satisfying ITAR-FREE regulations. Conformal coating (PARYLENE-C) has been applied to the board, and a shielding case made of 0.5t aluminum has been utilized to address radiation and mitigate interference.

OBC / FSW

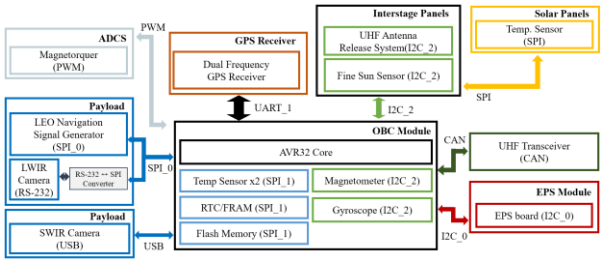

Figure 7: SPIRONE Data Interface

The communication interface buses of this CubeSat utilize SPI, I2C_0-CSP, I2C_2, CAN-CSP, PWM, USB Serial, and USART1. Detailed data interfaces can be found in Figure 7.

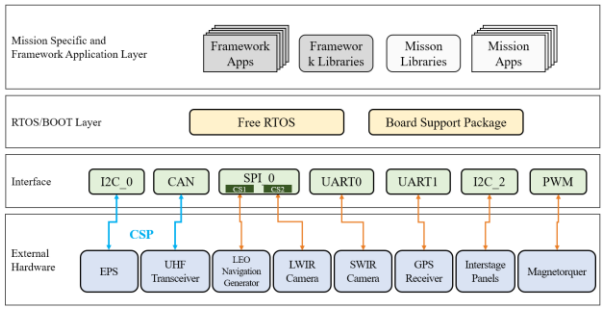

Figure 8: SPIRONE Software Architecture

The External Hardware and Interface layers represent hardware connections, while the RTOS/BOOT Layer and Mission-Specific and Framework Application Layer depict software structures. Each layer is interconnected organically, with data flowing sequentially from top to bottom or from the bottom to the upper layers.

The External Hardware layer represents hardware modules connected to the OBC. It includes subsystems and modules necessary for SPIRONE's operation and mission execution. The temperature sensor, RTC/FRAM, Flash Memory, Magnetometer, and Gyroscope are located internally within the OBC. The Interface layer represents interfaces within the OBC, with orange arrows indicating how each hardware component communicates through interfaces. Of particular note among the data interfaces is the inclusion of the CubeSat Space Protocol (CSP) interface in the CAN bus, through which the UHF Transceiver communicate using CSP. The RTOS/BOOT Layer comprises the operating system and BSP of the OBC. The operating system used for SPIRONE is FreeRTOS, utilizing the NanoMind A3200 (OBC) BSP provided by Gomspace. The Mission Specific and Framework Application Layer includes apps and libraries provided by the BSP, as well as additional apps and libraries added for mission execution. The libraries provided by the BSP contain various drivers, and mission execution tasks are included in the Mission APP and libraries.

Attitude determination / Control

For the precise execution of the CubeSat's mission, the role of the Attitude Determination and Control System (ADCS) is crucial. The ADCS consists of sensors for measuring attitude, actuators for responding to commands and altering attitude, and software for estimation and control. The attitude control system is divided into two modes: the angular velocity damping mode, which reduces the tumbling state speed of the CubeSat after release from the Pod, and the Nadir pointing mode, which maintains a stable attitude facing the Earth for scientific and technical mission objectives.

The angular velocity damping mode stabilizes the CubeSat using a B-dot controller based on the rate of change of the measured magnetic field values, and operation ceases when the angular velocity falls below 0.7 deg/s. The Nadir pointing mode utilizes a Linear Quadratic Regulator (LQR) controller to maintain the attitude of the CubeSat towards the Earth. This mode assumes the satellite's body frame coordinates are close to 0 degrees, employing a linearized approximation of the satellite's nonlinear mathematical model when designing the LQR controller.

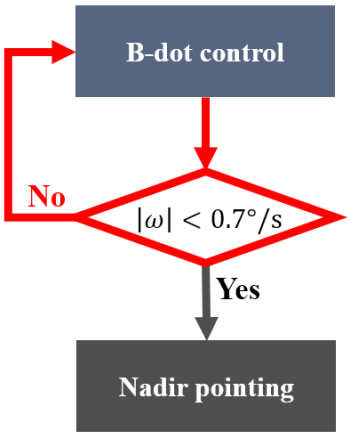

Figure 9: ACS Algorithm Design

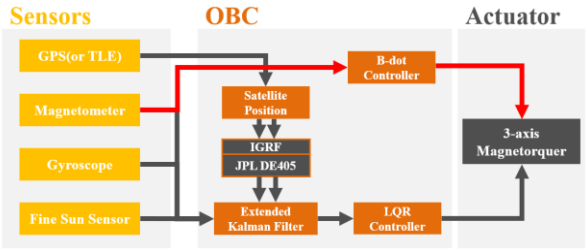

Figure 10: ADCS Software Block Diagram

To obtain information about the satellite's state, both position and attitude measurement sensors are required. This CubeSat utilizes the matterwave GPS antenna for receiving orbital position information. This sensor is connected to the OBC via USART and estimates the satellite's position using received GPS data.

For attitude measurement, sensors such as sun sensors, gyroscopes, and magnetometers are adopted to meet the size, weight, and power consumption requirements according to the 2U form factor. Sun sensors are attached to all five sides of the satellite except the nadir side and are connected to the OBC via the I2C interface. Each sun sensor has a 45° Field of View (FOV), and the positions and fields of view of each sensor are illustrated in Figure 11 to aid understanding.

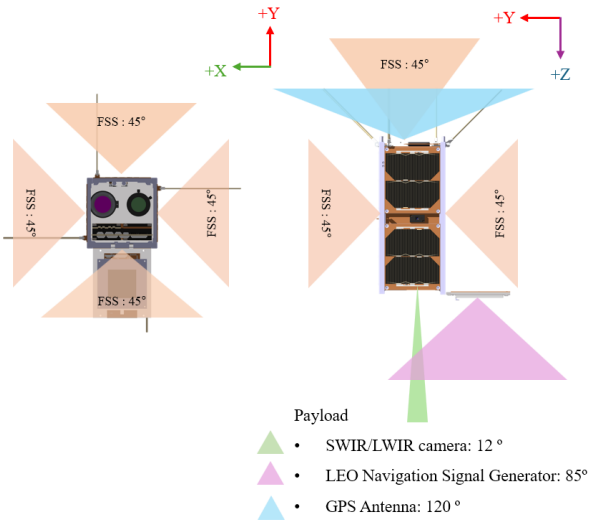

Figure 11: ADCS Sensors and Antenna FOV

Moreover, this CubeSat utilizes the Honeywell HMC5843 magnetometer sensor and the Invensense MPU-3300 gyroscope as attitude measurement sensors. Each sensor is integrated into the OBC and communicates via the I2C interface. Following the completion of the angular velocity damping mode, the initial attitude estimation using the TRIAD method employs the FSS and the magnetometer sensor. In the Nadir pointing mode, the attitude values are obtained using the FSS, magnetometer sensor, and gyroscope sensor.

CubeSats requiring precise attitude control typically employ reaction wheels and magnetorquers. Reaction wheels offer precise attitude control due to high torque output, but consume more power and have a higher risk of failure due to rotating nature. On the other hand, magnetorquers provide lower torque output, consume less power, and have a simpler drive mechanism, resulting in lower failure rates. This CubeSat has selected magnetorquers as magnetorquers satisfy the attitude system requirements and enable stable mission operations. The magnetorquers consist of one Gen1 Cubecoil and two Gen2 CROO3 units from CubeSpace, utilizing the PWM interface for communication with the OBC. The specifications of the magnetorquers are detailed in Table 4.

Table 4: Magnetorquer Specification

CubeTorquer GEN1 CubeCoil Double & GEN2 CR0003 (CubeSpace)		
Parameter	Value	Unit
PWM Voltage	3.3	V
Dipole Moment (Z-Axis)	0.18	Am^2
Dipole Moment (X, Y-Axis)	0.21	Am^2
Resistance (Z-Axis)	35-37	Ohm
Resistance (X, Y-Axis)	66.5	Ohm

The angular velocity damping algorithm utilizes the B-dot algorithm, which controls using changes in the magnetic field in body coordinates and the magnetic field created within the satellite. For gyro measurements, the rate of change of the magnetic field measured in space and the rate of change of the magnetic field measured in the space environment are used to determine. When the angular velocity falls below 0.7 deg/s, the angular velocity damping algorithm stops by applying a moving average. Since the input of the magnetorquer affects the magnetic field measurement, simultaneous use of the magnetometer sensor and magnetorquer is not feasible. Therefore, the magnetic field measurement is conducted for 2 seconds, followed by 2 seconds of magnetorquer operation. The angular velocity damping algorithm can be represented graphically in Figure 12 and expressed mathematically in Equation (1). The equation for angular velocity estimation during angular velocity damping is given by Equation (2).

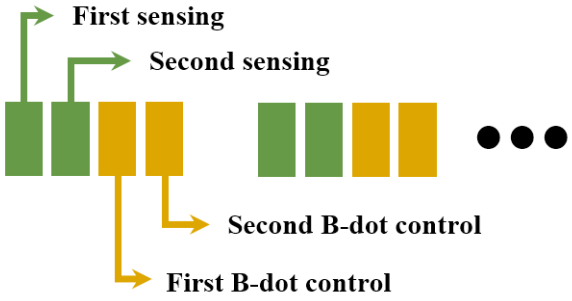

Figure 12: Angular Rate Damping Algorithm

$$u = -K_{bdot} \cdot \frac{B_k - B_{k-1}}{\Delta t},\ K_{bdot} > 0 \quad (1)$$

B: Mangetic field measurement

$$\dot{\vec{B}}_E = \dot{\vec{B}}_B + \vec{\omega} \times \vec{B}_B \quad (2)$$

The attitude determination utilizes three sensors: the magnetometer sensor, gyroscope, and FSS. The FSS is not used during eclipse. Since the input of the magnetorquer affects the magnetic field measurement, simultaneous use of the magnetometer sensor and magnetorquer is not feasible. Therefore, the process involves one-second magnetic field measurement using the magnetometer sensor followed by one-second magnetic field control using the magnetorquer, repeated in a loop. The utilization of sensors according to the solar period and eclipse is shown in Table 5.

Table 5: Sensor Utilization by Solar Period / Eclipse

Sensor	Solar period		Eclipse	
	Estimation	Control	Estimation	Control
Sun Sensor	O	O	X	X
Magnetometer	O	X	O	X
Gyroscope	O	O	O	O

Structure / Thermal

The SPIRONE CubeSat predominantly utilizes commercial-off-the-shelf products with established flight heritage in space. However, for the LEO navigation signal generator, the plan is to develop it in-house and conduct broadcasting and validation in low Earth orbit. Therefore, before the fabrication process, structural and thermal analyses through simulation are essential to assess its survivability in the launch environment and the space environment.

The SPIRONE CubeSat is planned to be a 2U CubeSat, but since the size of the Pod is 3U, a 1U dummy mass will also be included for launch. There exists a requirement that the maximum mass for the 3U configuration must not exceed 6 kg. Considering an additional margin of 10%, the calculated total weight is approximately 3.4 kg, securing a 43.3% mass budget.

The SPIRONE CubeSat, along with a 1U dummy, will be released from a 3U-sized Pod. Therefore, positioning the center of mass of the entire satellite, including the 1U dummy, at the center of the Pod can reduce tumbling upon release. The configuration of the SPIRONE CubeSat and Dummy to be placed inside the Pod is illustrated in Figure 13, while the overall center of mass and moments of inertia of the satellite are detailed in Table 6.

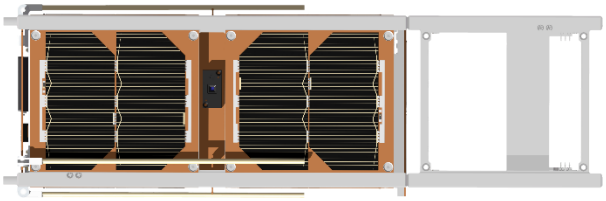

Figure 13: SPIRONE Cubesat (2U) + Dummy (1U)

Table 6: Satellite Center of Mass and Moments of Inertia

		Initial Mode
Center of Mass	G_X	-4.126 mm
	G_Y	-2.646 mm
	G_Z	+0.281 mm
Moment of inertia	I_X	0.023 kg ·m^2
	I_Y	0.023 kg ·m^2
	I_Z	0.005 kg ·m^2
	I_{XY}	-4.43x10^{-5} kg ·m^2
	I_{XZ}	2.73x10^{-6} kg ·m^2
	I_{YZ}	-1.33x10^{-4} kg ·m^2

The S-Band antenna deployment mechanism underwent direct 3D modeling to determine the deployment method. Due to design requirements that prohibit the use of explosive separation devices, the CubeSat utilizes the commonly adopted nichrome wire-cutting method as the restraint and separation mechanism for CubeSat deployment, rather than explosive devices. The nichrome wire-cutting method involves attaching the restraint to the target structure and then cutting through the wire using the heated nichrome wire to release the restraint. This is generally the most commonly used approach, and it was deemed suitable as the required operating current of around 1.1A to 3A is considered appropriate.

The chosen method offers several advantages, such as low cost and relatively easy fabrication. However, it requires measures to prevent wire slackening, and when produced for one-time use, it faces limitations in verification and testing. Therefore, a multi-use approach is recommended whenever possible. The selected wire is thin yet durable, lightweight, resilient, and flexible. Additionally, the use of glue is being considered to prevent the loosening of knots. The S-Band antenna deployment mechanism has been designed to utilize a hinge structure with torsion springs to enable a 180-degree deployment. The S-Band antenna deployment unit is designed to be mounted on the payload support structure, as shown in Figure 14.

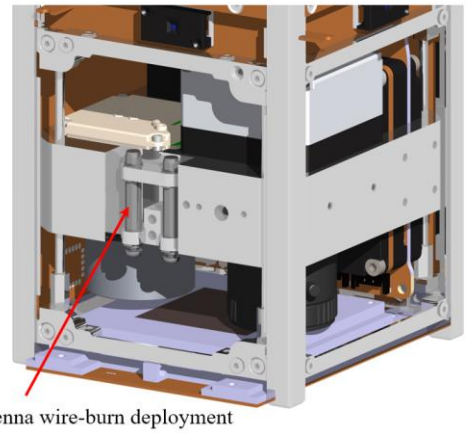

Figure 14: SPIRONE Lower Section 3D Design

Before CubeSats are launched into space, it's crucial to ensure that the structures and modules can withstand extreme conditions during the launch period.

Throughout the launch period, CubeSats remain housed within the Pod, requiring consideration of such launch environments. Therefore, the upper and lower surfaces of the CubeSat are fixed to the Pod, while the corner rails are subjected to X and Y-axis movement restrictions. Using ANSYS, structural analyses including Resonance Survey, Random Vibration, and Quasi-Static Analysis were conducted to verify compliance with the launch vehicle requirements.

Figure 15: Structural Analysis Results

Thermal analysis was conducted using Thermal Desktop software, which simulated the operational orbit, applying radiation and conduction effects. The orbit was set considering an altitude of 600km and a 12:30 Local Time of Ascending Node (LTAN). Simulations were performed for initial mode, safe mode, and technical mission mode under worst hot/cold environments. The operational status of critical modules for each specific operational mode is presented in Table 7, while parameter settings for worst hot/cold conditions are detailed in Table 8.

Table 7: Critical Module Operation Status by Operating Mode

Module	Initial	Safe	Technical mission
LEO NSG	X	X	O
OBC	O	O	O
Battery	O	O	O
LWIR	X	X	X
SWIR	X	X	X
GPS receiver	X	X	O
UHF transceiver	O	O	O
Note		Min Heat	Max Heat

Table 8: Parameter Settings for Worst-Case Hot/Cold Conditions

Parameter	Worst cold	Worst hot
Altitude	600 km	
Inclination	97.8º	
R.A.A.N	244.2123º	
Eccentricity	0.0012788	
Solar Constant	1321 (W/m^2)	1412 (W/m^2)
Albedo	0.18	0.55

As a result of the thermal analysis conducted under the aforementioned conditions, it was confirmed that each module operates within the normal temperature range specified in the datasheet for the space orbit environment. Additionally, the battery temperature was found to be within the normal range.

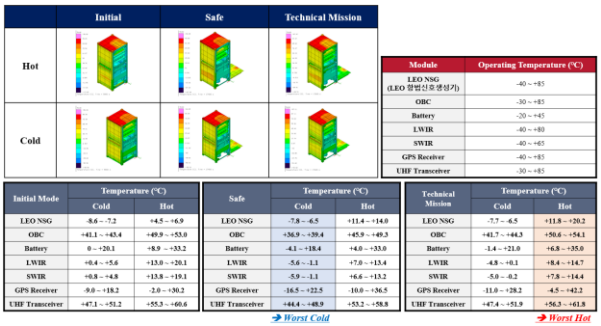

Figure 16: Thermal Analysis Results

Power

The power system of the CubeSat consists of solar panels, the Electrical Power System (EPS), and lithium-ion batteries. Gomspace's P110 solar panels, NanoPower P31u board, and NanoPower BP4 batteries are utilized. The battery uses a basic Li-ion battery of 4V. Solar panels serve as the primary energy source for the CubeSat, with plans to mount 2 panels each on the ±X and ±Y axes, 1 panel on the +Z axis, and 0.5 panels on the -Z axis. Additionally, a custom solar panel will be manufactured to accommodate the GPS antenna and FSS on the -Z axis. The overall configuration of the power system is illustrated in Figure 17, with the diagram provided in Figure 18.

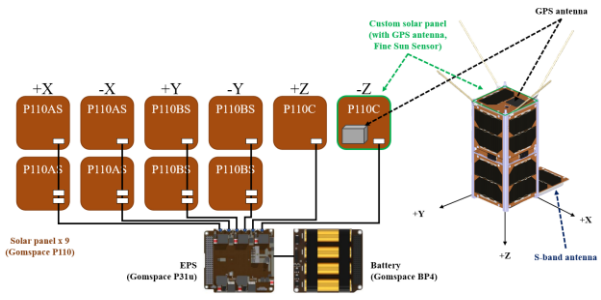

Figure 17: Power System Configuration

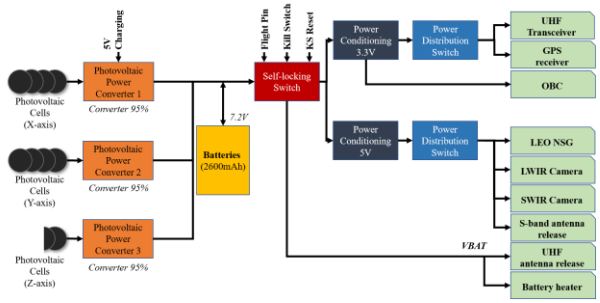

Figure 18: Power System Diagram

During satellite operation in orbit, a power analysis was conducted to analyze the trend of energy charge and discharge, ensuring an adequate energy supply for mission execution. In the power generation analysis, modeling was performed using parameters of the planned solar panels, and the actual power production of the satellite was analyzed. Additionally, power consumption was calculated based on operational scenarios, and simulations were conducted using the power production and consumption in orbit. Based on these results, the battery status of the satellite was verified to be compatible with mission requirements.

Additionally, a power stability analysis during tumbling state after satellite deployment was conducted to review the performance of the power system under various conditions. This allowed for an assessment of the satellite's survivability. The model parameters for the P110 solar panel are presented in [Table 9, Table 10]. The given solar cell model, AZURSPACE's 3G30A, consists of two cells connected in series to form the P110. The nominal solar irradiance and temperature for modeling parameters are 1367 W/m^2 and 28 ℃, respectively.

Table 9: Solar Cell Modeling Parameters: Electrical Data

Parameter	Value	Unit
Aerage Open Circuit (V_{oc})	2690	mV
Aerage Short Circuit (I_{sc})	519.6	mA
Voltage at max. Power (V_{mp})	2409	mV
Current at max. Power (I_{mp})	502.9	mA

Table 10: Solar Cell Modeling Parameters: Temperature Gradients

Parameter	Value	Unit
Open Circuit Voltage ($\Delta V_{oc}/\Delta T\uparrow$)	-6.2	mV/degC
Short Circuit Current ($\Delta I_{sc}/\Delta T\uparrow$)	0.36	mA/degC
Voltage at max. Power ($V_{mp}/\Delta T\uparrow$)	-6.7	mV/degC
Current at max. Power ($I_{mp}/\Delta T\uparrow$)	0.24	mA/degC

In order to obtain simulation results similar to real-world scenarios, the solar panel was modeled to calculate its power output. By modeling the solar cells using equivalent circuit modeling, current-voltage curves can be obtained based on temperature and solar irradiance. These curves allow for the identification of the Maximum Power Point (MPP), and the power output is defined as the power generated at the MPP. The characteristic equation of a solar cell can be expressed as follows.

$$I_0 = \frac{I_{sc,n} + K_I \Delta}{\exp((V_{oc,n} + K_V \Delta_T)/aV_t) - 1} \tag{3}$$

$$R_{p,\min} = \frac{V_{mp}}{I_{sc,n} - I_{mp}} - \frac{V_{oc,n} - V_{mp}}{I_{mp}} \tag{4}$$

$$I_{pv,n} = \frac{R_p + R_s}{R_p} I_{sc,n} \tag{5}$$

$$I_{pv} = (I_{pv,n} + K_I \Delta_T) \frac{G}{G_n} \tag{6}$$

$$R_p = \frac{V_{mp}(V_{mp} + I_{mp}R_s)}{\left\{ V_{mp}I_{mp} - V_{mp}I_0 \exp\left[\frac{V_{mp} + I_{mp}R_s}{N_s a} \frac{q}{kT} \right] + V_{mp}I_0 - P_{\max,e} \right\}} \tag{7}$$

The solar panel's resistances (R_s, R_p) were calculated using the solar panel simulation flowchart shown in Figure 19. The input temperature and solar irradiance were set to nominal values, with an initial value of 1 utilized for R_s.

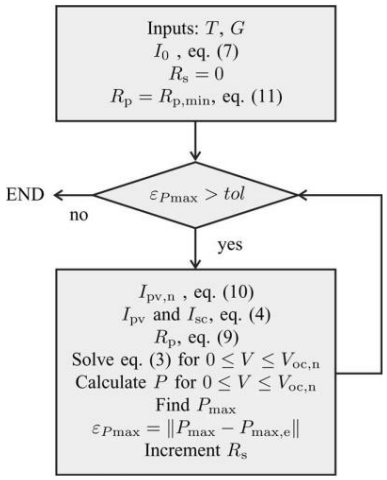

Figure 19: Solar Panel Simulation Flowchart

Based on these steps, the generated power before and after the deployment of the S-Band antenna for the CubeSat was calculated and presented in Table 11.

Table 11: Average Power Generation

	Avg Power Gen.
Power Gen. (Pre S-band deployment)	2.68 W
Power Gen. (Post S-band deployment)	3.27 W

The power consumption for each operational mode was also calculated. The power load from the bus components was computed using Equation (8), and the total value was determined considering a contingency of 10% and an efficiency of 90%, as shown in Table 12.

$$\sum_{\text{all bus units}} \{\text{power(mode)} \times (1+\text{contingency})/\text{efficiency}\} \quad (8)$$

Table 12: Power Consumption During Solar Period and Eclipse

	Power Consumption [W]	
	Solar period	Eclipse
Initial	1.25	3.08
Standby (S-Band pre/post)	1.32/1.87	3.15/3.70
Safe	0.73	2.56
Technical mission	11.46	13.29
Scientific mission	6.27	X
Communication	4.84	6.68
Hibernation	0.79	2.53

The results of the power margin, considering both power generation and consumption, are summarized in Table 13. This accounts for a power margin with considerations including an 85% efficiency for power generation converters, a 10% contingency for power consumption, a 90% efficiency for converters, along with other losses such as 1% harness loss and 5% battery loss. It's noted that the power margin is positive for all modes.

Table 13: Power Margin

	Mode	Power Gen [W]	Power Draw [W]	Power Margin [%]
S-Band pre	Standby	2.7	1.89	21.3
	Safe		1.30	76.4
S-Band post	Standby	3.3	2.44	14.8
	Safe		1.30	115.6
	Technical		2.46	14.2
	Scientific		2.06	36.4
	Communication		2.06	36.5

Communication

The primary purpose of the communication subsystem is smooth communication with ground stations, followed by sending observation and satellite status data to the ground. The On-Board Computer (OBC) receives information from each subsystem and transmits it through the transceiver. The transceiver operates in the UHF-band range for communication, transmitting data from the satellite to the ground as downlink and receiving commands from the ground to the satellite as uplink, also using the UHF-band (430-440 MHz). The transmission power is set at 2W, the downlink data rate is 9,600 bps and the link budget is 5.23 dB, while the uplink data rate is 1,200 bps and the link budget is 25.81 dB.

The conceptual diagram of the overall communication system is shown in Figure 20. The communication protocol will utilize the AX.25 protocol and be implemented using commercial modules. Specifications of the communication modules and antennas to be used in the communication system are presented in Table 14. Upon reviewing Table 14, it can be observed that all communications occur in the amateur frequency range.

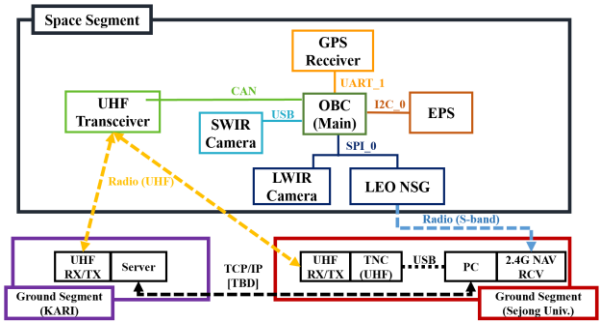

Figure 20: Network Topology

Table 14: Communication Module and Antenna Specifications

		Specification
UHF Transceiver	Frequency Band	430 ~ 440 MHz
	Transmit Power	24 ~ 30 dBm
	Modulation Method	GFSK / GMSK
	Data Transfer Rate	100 ~ 38,400 bps
UHF Antenna	Frequency Band	400 ± 5 MHz / 435 ± 5 MHz
	Gain	1.6 dBi to -1 dBi
	Bandwidth	10 MHz

The downlink includes both beacon signals and mission data. Starting with the beacon signals, they contain fundamental information about the satellite's orbit, attitude, and power status. The beacon signals will be operated in two modes: simple beacon and full beacon.

The simple beacon, broadcast every 10 seconds, includes information regarding time, position, and power modules (battery mode, battery voltage), with a data size of 360 bits. The full beacon, broadcast every 30 seconds, includes additional details such as time, position, power modules, satellite attitude, current mode, temperature, and deployment status, with a data size of 1,264 bits.

Additionally, the downlink contains mission data. The scientific mission of this CubeSat is to detect oceanic plastic. It is planned to conduct missions within a radius of approximately 2041.18km in the areas of the Korean Peninsula, the Pacific Ocean, and the Atlantic Ocean. Figure 21 illustrates the area where the IR camera array collects mission data.

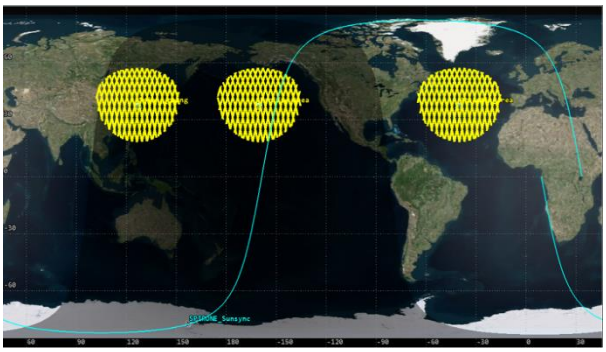

Figure 21: Mission Data Collection Area

The composition of mission data per cycle is outlined in Table 15. RAW files generated by the IR camera array are compressed to 1/8 of their size, resulting in a compressed file size of 32.5 Kbytes. GPS data consists of ECEF data and TOW data, totaling 0.004 Mbytes. Mission data collection time is configured using STK simulation for a sun-synchronous orbit at an altitude of 600km, with a total mission data size of 3.674 Mbytes.

Table 15: Mission Data Design

	GPS	IR Camera Array
Data Composition per Cycle	NAV-SOL: Header (2*char) TOW (2*Uint) ECEF_X (int) ECEF_Y (int) ECEF_Z (int) Quaternion Data (3*float)	SWIR: 17,920byte LWIR: 15,360byte *JPG format 1/8 Compression Image Size: 33,280byte: 32.5 KB
Data Collection Area	Korean Peninsula Sea, Pacific, Atlantic	
Collection Time	Each Area: Max. 34.9 mins = 2095.3 secs	
Data Collection Interval	Max. 18.12 secs	
Collected Data	(22+12)byte*(2095.3s / 18.12s)/1024^2 : 0.004Mbyte	33,280byte*(2095.3s /18.12s)/1024^2 : 3.670 Mbtye
Total Data (Per Day)	3.674 Mbyte	

Housekeeping data refers to periodically stored status data of the CubeSat in storage. SPIRONE's housekeeping data will store full beacon signals at 1-minute intervals in flash memory for the past 30 days. Additionally, it will update the data using a ring buffer structure. With each full beacon data size at 158 bytes, storing it at 1-minute intervals for 30 days would require 6.51 Mbytes. The cut-off angle at Sejong University's ground station is set to 5 degrees. Utilizing the communication availability times from Table 16, the maximum daily data transmission capacity is calculated, and based on this, the transmission times for mission data and housekeeping data are determined in Table 17. Part of the compressed mission data deemed appropriate can be requested via telecommand to receive as RAW data files. The size of one RAW file photo generated by the IR camera array is 260 Kbytes, with a transmission time of approximately 113 seconds.

Table 16: Communication Time and Data Transfer Prediction

Frequency Range	Max. Data Rate (Mbyte/s)	Daily Comm. Frequency	Daily Comm. Time (sec)	Daily Max Data Transfer (Mbyte/s)
UHF	0.0023	4.267	2,095.3	3.674

Table 17: Data Transmission Time

	Mission Data	Housekeeping Data
Daily Data Collection	3.674 Mbyte	0.217 Mbyte
Transmission Time	About 0.76 days	About 0.045 days
Total Daily Data Transmission Time	About 0.81 days ≈ 19.44 hours	

Telemetry refers to the data transmitted from the satellite to the ground station, including both housekeeping data and mission data. By utilizing the current packet index and the total packet index, the ground station can identify any missing telemetry transmissions and send retransmission requests. The telemetry is transmitted using CSP and AX.25 specifications, with the payload size set to match that of the housekeeping data. Any remaining space in the data packet is filled with 0xFF. Telecommands, on the other hand, are commands sent from the ground station to the satellite, encompassing actions such as system resets, mode transitions, and requests for satellite information. Types of commands include system reset, antenna deployment, mode transitions, satellite information requests, and configuration changes. The structure of telemetry and telecommands is shown in Figure 22.

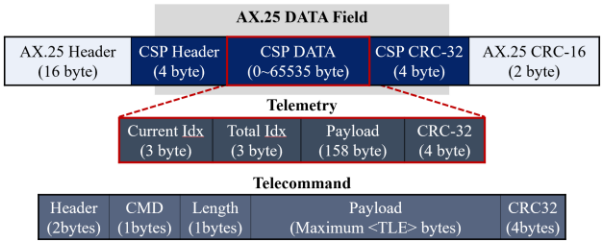

Figure 22: Telemetry and Telecommand Architecture

Ground station

Ground stations receive beacon signals from satellites in orbit to assess the satellite's status, relay commands to the satellite, and receive mission data collected by the satellite. Ground stations must continuously monitor the satellite's position and orbit information, as well as assess the current status and communication capability of the satellite. Sejong University, currently developing the CubeSat, completed the construction of its ground station in 2023. Sejong University plans to operate the SPIRONE CubeSat in collaboration with the KARI, which is supporting the ground station. KARI serves as a backup ground station in case of any issues with Sejong University's ground station operations. Figure 23 depicts the structure of Sejong University's ground station.

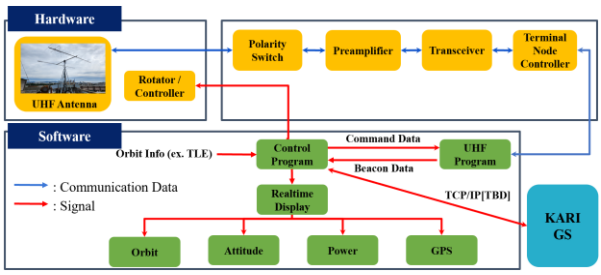

Figure 23: Sejong University Ground Station Layout

The CubeSat's planned operating frequency ranges from 430 to 440 MHz for both uplink and downlink communications. Ground stations require corresponding transceiving equipment for this purpose. To facilitate this, outdoor equipment such as antennas, antenna rotators, polarity switches, and preamplifiers have been installed, while indoor equipment including transceivers, rotator controllers, TNCs, and ground station PCs has also been set up.

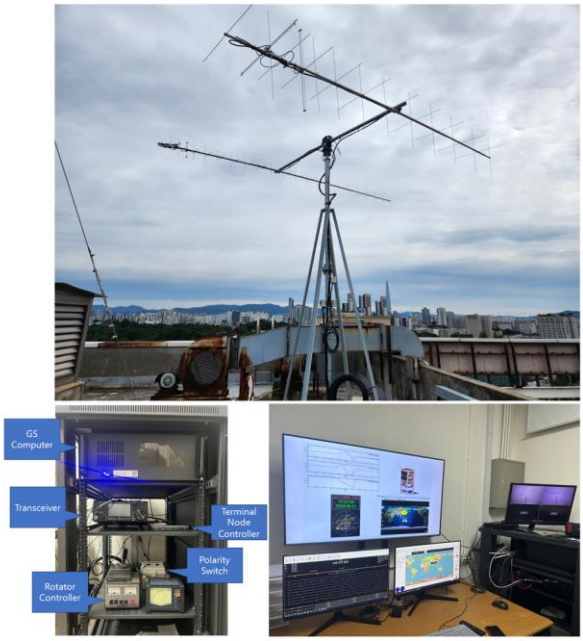

Figure 24: Current Status of Sejong University Ground Station Development

To verify the proper functioning of both ground station hardware and software, SDR#, Ham Radio Deluxe, and WXtoImg were utilized to receive images of the Korean Peninsula from the NOAA-19 satellite (from 2023-05-22 20:26:25 to 2023-05-22 20:37:26). Additionally, beacon signals were received from the SNUGLITE-I satellite.

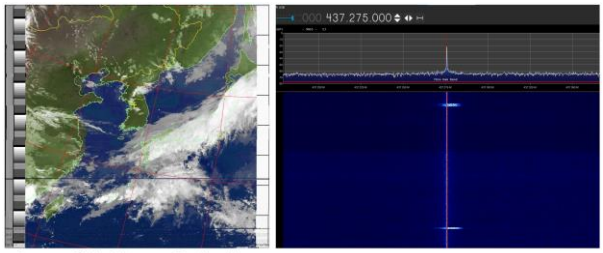

Figure 25: Data Received for Ground Station System Verification

The ground station software is responsible for verifying the satellite's orbit and position, controlling the antenna to track the CubeSat, and providing users with various information about the satellite's mission through an interface. The operation of the ground station software is anticipated to be as depicted in Figure 26, with separate installations for control and communication software.

The control software utilizes the Ham Radio Deluxe program, which leverages the orbit information of the CubeSat to calculate its position and velocity. This enables the determination of the CubeSat's

communicable time and the visibility of GPS satellites. By calculating the elevation and azimuth angles of the satellite during communicable time, the control software can perform antenna control.

The communication software functions to efficiently process signals during transmission and reception between the CubeSat and the ground station. It will be developed in-house, and the communication software will visualize the received beacon data in real-time as an interface during communication with the CubeSat. It will also receive and store mission data and housekeeping data.

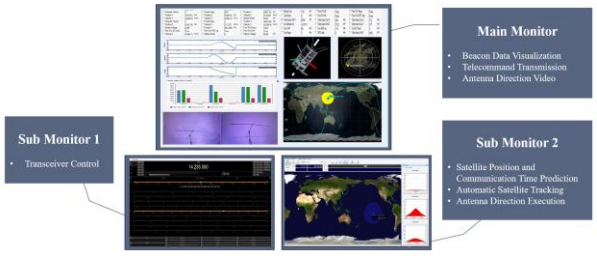

Figure 26: Ground Station Software Operation Projection

CONCLUSION

This paper provides an overview of the development of the SPIRONE CubeSat being developed at Sejong University. This CubeSat aims to develop and validate a LEO navigation signal generator as its technical mission and to observe marine plastic debris using an IR camera array as its scientific mission. The development schedule has completed the SDR, PDR, and CDR stages, with the TRR and FRR stages planned before the scheduled launch on the Nuri rocket in November 2025. Additionally, risks that may arise at each development stage and post-launch are managed for each subsystem. After the development of each system, module integration will be conducted before the TRR, followed by the first space environment test for the EQM and the second space environment test for the FM. Finally, preparations for space operation will be completed through a Far-field test.

ACKNOWLEDGMENTS

This work was supported by the National Research Foundation of Korea (NRF) grant funded by the Korea government (MSIT) (NRF-2022M1A3C2014567). Additionally, the authors would like to express their gratitude for the support provided by the Future Space Navigation & Satellite Research Center through the National Research Foundation funded by the Ministry of Science and ICT, the Republic of Korea (2022M1A3C2074404)

REFERENCES

1. ″SpaceX satellite signals used like GPS to pinpoint location on Earth”, https://news.osu.edu/spacex-satellite-signals-used-like-gps-to-pinpoint-location-on-earth/
2. Zizhong Tan, ″Positioning Using IRIDIUM Satellite Signals of Opportunity in Weak Signal Environment″, Electronics, 2019
3. Mohammad Neinavaie et al, ″Exploiting Starlink Signals for Navigation: First Results″, 2021 ION GNSS+ Conference, 2021
4. González, A., Rodriguez, I., Navarro, P., Sobrero, F., Carbonell, E., Calle, D., & Fernández, J. (2022, September). Leo satellites for PNT, the next step for precise positioning applications. In Proceedings of the 35th International Technical Meeting of the Satellite Division of The Institute of Navigation (ION GNSS+ 2022) (pp. 2573-2581).
5. Prol, F. S., Ferre, R. M., Saleem, Z., Välisuo, P., Pinell, C., Lohan, E. S., ... & Kuusniemi, H. (2022). Position, navigation, and timing (PNT) through low earth orbit (LEO) satellites: A survey on current status, challenges, and opportunities. IEEE Access, 10, 83971-84002.
6. https://www.cnn.com/2023/04/17/world/plastic-pollution-ocean-ecosystems-intl-climate
7. ″ Locata”, https://www.locata.com/technology/locata-tech-explained/locatas-inventions/
8. Wilson, A. N., Gupta, K. A., Koduru, B. H., Kumar, A., Jha, A., & Cenkeramaddi, L. R. (2023). Recent advances in thermal imaging and its applications using machine learning: A review. IEEE Sensors Journal, 23(4), 3395-3407.
9. Qin, B., Zhu, Y., Zhou, Y., Qiu, M., & Li, Q. (2023). Whole-infrared-band camouflage with dual-band radiative heat dissipation. Light: Science & Applications, 12(1), 246.
10. Kim, O. J., Shim, H., Yu, S., Bae, Y., Kee, C., Kim, H., ... & Choi, Y. (2020). In-orbit results and attitude analysis of the snuglite cube-satellite. Applied Sciences, 10(7), 2507.